# Theoretical and experimental serviceability performance of SCCs connections

Ali Akbar Maghsoudi*

*Department of Civil Engineering, University of Kerman & International Center for Science,
High Technology & Environmental Sciences, Kerman, Iran*

**Abstract.** The Self Compacting Concrete, SCC is the new generation type of concrete which is not needed to be compacted by vibrator and it will be compacted by its own weight. Since SCC is a new innovation and also the high strength self compacting concrete, HSSCC behavior is like a brittle material, therefore, understanding the strength effect on the serviceability performance of reinforced self compacting concretes is critical. For this aim, first the normal and high strength self compacting concrete, NSSCC and HSSCC was designed. Then, the serviceability performance of reinforced connections consisting of NSSCC and HSSCC were investigated. Twelve reinforced concrete connections ($L = 3$ m, $b = 0.15$ m, $h = 0.3$ m) were simulated, by this concretes, the maximum and minimum reinforcement ratios $\rho$ and $\rho'$ (percentage of tensile and compressive steel reinforcement) are in accordance with the provision of the ACI-05 for conventional RC structures. This study was limited to the case of bending without axial load, utilizing simple connections loaded at mid span through a stub ($b = 0.15$ m, $h = 0.3$ m, $L = 0.3$ m) to simulate a beam-column connection. During the test, concrete and steel strains, deflections and crack widths were measured at different locations along each member. Based on the experimental readings and observations, the cracked moment of inertia ($I_{cr}$) of members was determined and the results were compared with some selective theoretical methods. Also, the flexural crack widths of the members were measured and the applicability for conventional vibrated concrete, as for ACI, BS and CSA code, was verified for SCCs members tested. A comparison between two Codes (ACI and CSA) for the theoretical values cracking moment is indicate that, irrespective of the concrete strength, for the specimens reported, the prediction values of two codes are almost equale. The experimental cracked moment of inertia ($I_{cr}$)$_{exp}$ is lower than its theoretical ($I_{cr}$)$_{th}$ values, and therefore theoretically it is overestimated. Also, a general conclusion is that, by increasing the percentage of $\rho$, the value of $I_{cr}$ is increased.

**Keywords:** SCCs; connection; neutral axis; crack width; cracked moment of inertia; serviceability

## 1. Introduction

Self Compacting Concrete, SCC is a new type of concrete, which has generated tremendous interest since initial development in Japan by Okamura in the 1980s in order to reach durable concrete structures (Okamura 1997).

Since that time, Japanese contractors have used SCC in different applications. In contrast with the Japan, research in Europe and American started latter (Skarendahl and Petersson 2001). SCC offers

---

*Corresponding author, Associate Professor, E-mail: Maghsoudi.a.a@mail.uk.ac.ir, al_maghsoudi@yahoo.com

both cost and quality improvements over conventional concretes. The high fluidity of SCC certainly contributes to good placement of concrete in all sections of the formwork but in cases of densely reinforced cross sections the maximum aggregate grain size has the crucial impact.

Placement times are decreased and labor requirements are lowered (Khayat 1999, Saria *et al.* 1998). However, more theoretical and experimental research is required to understand the effect of this type of concrete on structural elements.

The objective of this research study is to provide information on serviceability stage of the important elements such as connections in reinforced concrete, RC structures made of NSSCC and HSSCC. The literature review is indicating that no research report is available on this field. However, the reports are available on conventional reinforced concrete connections (Burns and Siess 1962, Joint ACI-ASCE committee 352 2004, Ernst 1957, ACI 2005, Robertson *et al.* 2002).

The load-deformation behavior of RC members made of SCCs loaded to failure, particularly the, cracks propagations, that develops at the connection of a beam to a column in a frame is investigated and reported. Also the parameters contributing to the serviceability of beam-column connections for this new type of concrete, which is important when a structure is under the service loading, are investigated. This study was limited to the case of bending without axial load, utilizing simple beams loaded at mid span through a stub to simulate a beam-column connection. The dimensions and type of test selected here, are similar to the work reported by Burns and Siess (1962) for normal concrete in RC structures.

High strength concrete, HSC provides a better solution to reduce sizes and weights of concrete structural elements (ACI committee 363 1992, Nilson 1987, Swamy 1987). The reduction in cross sectional area of concrete members also reduces the moment of inertia, $I$, of the members. This necessitates the investigation of the impact of reduction on deflection of beams under service load. The effective value of $I$ changes along the beam span from a maximum value of $I_g$ for un-cracked (gross) sections to a minimum value of $I_{cr}$ for the fully cracked (transformed) sections. The variation of $I$ along the beam span not only makes the deflection calculation lengthy and tedious but also, its accuracy is questionable while considering HSSCC. Hence, in a cracked member, it is important to provide a smooth continuous transition between $I_g$ and $I_{cr}$, over the entire length of a simply supported member. For conventional concrete, the ACI 318-2004 (ACI 2005) since 1971 recommends the use of the following expression for the calculation of the effective moment of inertia $I_e$

$$I_e = \left(\frac{M_{cr}}{M_a}\right)^3 I_g + \left[1 - \left(\frac{M_{cr}}{M_a}\right)^3\right] I_{cr} \tag{1}$$

A lack of information regarding the structural performance of SCC is one of the main barriers to its acceptance in the construction industry. However, recently, SCC has gained wide use in many countries for different applications and structural configurations (Skarendahl and Petersson 2001, Khayat 1999, Saria *et al.* 1998, Khayat *et al.* 2001, Yurugi 1998, Sonebi and Bortos 2001, Mohammad *et al.* 2006, Pateli *et al.* 2004). Limited published studies dealing with the structural performance of SCC demand initiation of new research especially while considering the serveciability of the SCC reinforced connections.

When the strength of concrete gets higher, some of its characteristics and engineering properties become different from those of normal-strength concrete (Carrasquillo *et al.* 1981, Mansur *et al.* 1994). These differences in material properties may have important consequences in terms of the structural behavior and design of high strength concrete members. The design provisions contained in the major building codes are, in reality, based on tests conducted on conventional NSC. While

designing a structure using HSC, the designer particularly in the Southeast Asian region usually ignores the enhanced properties of concrete and possible changes in the overall response of the structure because of lack of adequate code guidance (Rashid *et al.* 2002).

A few limited studies have been made for conventional HSC (Bosco *et al.* 1990, Akbarzadeh Bengar 2004, Leslie *et al.* 1976, Maghsoudi and Akbarzadeh Bengar 2005, Ashour 2000). A dimensional analysis was proposed by Bosco *et al.* (1990) to compute the minimum amount of reinforcement for HSC members in flexure. They tested thirty reinforced conventional high strength concrete beams with the cross section thickness $b = 150$ mm, and depth $h = 100$, 200, and 400 mm, respectively. They concluded that the minimum steel percentage tends to be inversely proportional to the beam depth, whereas the current standard codes suggest, for direct loading, values in depend of the beam depth. It follows that the formulas provided by the codes are inadequate, at least for conventional HSC. Maghsoud*i et al.* (Akbarzadeh Bengar 2004, Maghsoudi and Akbarzadeh Bengar 2005) reported on ductility of conventional HSC rectangular beams. Leslie *et al.* (1976) reported on 12 flexural tests of under reinforced rectangular beams with $f_c'$ ranging between 64 to 81 MPa. They concluded that, the currently used rectangular stress block (from the ACI building code) does not accurately predict the beam behavior when concrete strength exceeds 55 MPa. Pending further test results, the use of a triangular stress block seems prudent.

Ashour (2000), tested nine reinforced high-strength concrete beams to investigate the effect of concrete compressive strength and flexural tensile reinforcement ratio on load-deflection behavior and displacement ductility of cracked rectangular reinforced concrete beams. He concluded that the utilization of HSC, impacts the parameters involved in the deflection calculations. This includes concrete modulus of elasticity and cracked moment of inertia. He modified Eq. (1) for the effective moment of inertia. Also, assuming the permissible flexural crack widths for three different environmental conditions, the experimental values of strain and stress in steel and concrete are measured and reported.

The objective of this research is to investigate the effect strength of concrete and the percentage of tensile and compressive steel ratio (i.e., $\rho$ and $\rho'$) on the serviceability characteristics of SSC connections. The structural response throughout the loading regime was primarily captured in terms of the load deflection behavior. The serviceability characteristics of the test members were evaluated in terms of the crack width, deflection and stress in steel and concrete. Based on the experimental results, the cracked moment of inertia and crack width were compared with some selective theoretical methods, and the crack patterns in the connections are also presented.

## 2. Experimental program

### 2.1 Test specimens

In this investigation the results of twelve tested SCCs reinforced connections under three-point loads are considered for their serviceability performance. However, the ultimate and ductility considerations for some of such elements are reported by Mohamadi (2007), Gatteh (2006). Fig. 1 shows member dimensions, loading arrangements and reinforcement details, of the members. Eight connections were consisting NSSCC while the other four were consisting of HSSCC. Shear reinforcement was provided along the member length. Table 1 presents the detailed testing program. The NSSCC members are designated as S1-S8 whereas the HSSCC member is designated as SH1-
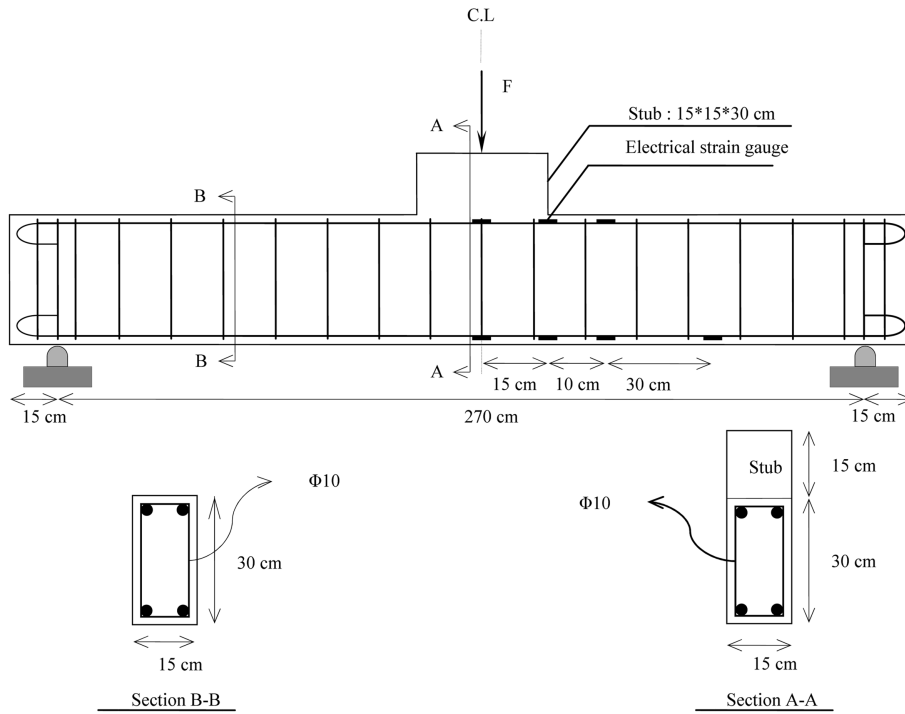
C.L

F

A

Stub : 15*15*30 cm

Electrical strain gauge

B

B

B

A

A

15 cm   10 cm   30 cm

15 cm                                    270 cm                                    15 cm

Φ10

30 cm

15 cm

Section B-B

Stub                15 cm

Φ10

30 cm

15 cm

Section A-A

Fig. 1(a) Beam-column connection details for SH series

C.L

F

4Φ12 (for S7)

A

Stub : 15*15*30 cm

4 Φ8@10 cm (for S7and S8)

Electrical strain gauge

B

B

B

A

A

15 cm   10 cm   30 cm

15 cm                                    270 cm                                    15 cm

Φ10

30 cm

15 cm

Section B-B

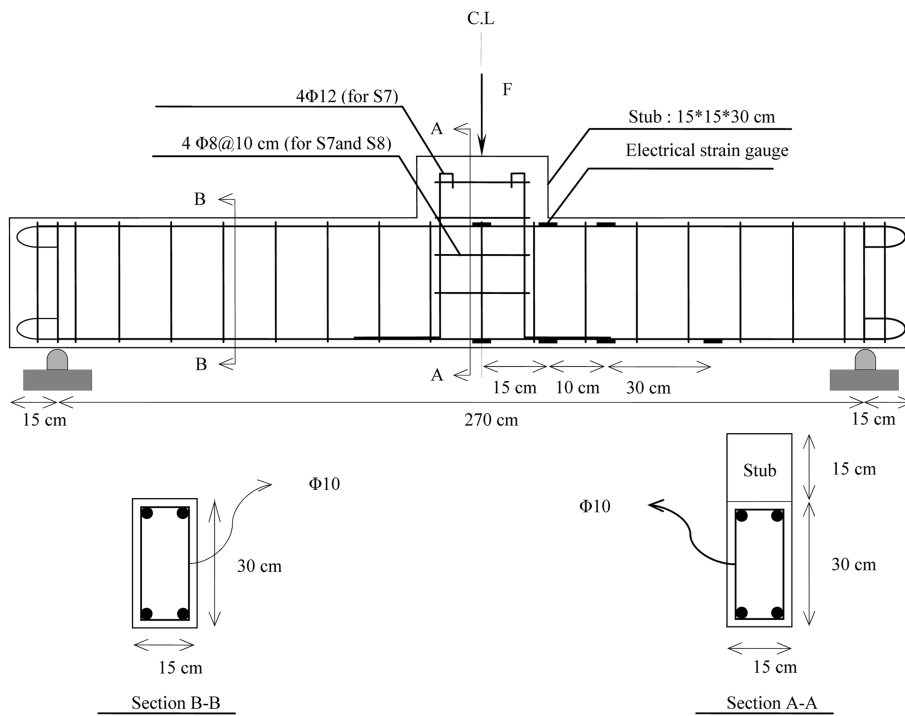Stub                15 cm

Φ10

30 cm

15 cm

Section A-A

Fig. 1(b) Beam-column connection details for S series

Table 1 Details of the experimental program parameters of tested members

| Member no. | $f_c'$ (MPa) | $f_y$ (MPa) | $d$ (mm) | $d'$ (mm) | $A_s$ | $\rho/\rho_b$ | $A_s'$ | $\rho$ | Stirrup in Beam | Tie in Column | $A_s$ in Column | $C$ (mm) | $\rho'/\rho$ |
|---|---|---|---|---|---|---|---|---|---|---|---|---|---|
| S1 | 30.2 | 398.1 | 263 | 33 | 2Φ10 | 0.13 | 2Φ10 | 0.41 | Φ10@15 | ----- | ----- | 32 | 1.00 |
| S2 | 29.7 | 373.6 | 260 | 34 | 2Φ16 | 0.27 | 2Φ12 | 1.03 | Φ10@15 | ----- | ----- | 32 | 0.56 |
| S3 | 28.1 | 401.9 | 258 | 38 | 2Φ20 | 0.33 | 2Φ16 | 1.61 | Φ10@10 | ----- | ----- | 32 | 1.00 |
| S4 | 30.8 | 401.9 | 258 | 36 | 2Φ20 | 0.38 | 2Φ20 | 1.61 | Φ10@15 | ----- | ----- | 32 | 0.64 |
| S5 | 32.7 | 370.0 | 257 | 39 | 2Φ25 | 0.56 | 2Φ18 | 2.52 | Φ10@10 | ----- | ----- | 31 | 0.52 |
| S6 | 30.7 | 400.0 | 256 | 39 | 2Φ28 | 0.66 | 2Φ20 | 3.16 | Φ10@15 | ----- | ----- | 30 | 0.45 |
| S7 | 27.6 | 373.6 | 267 | 31 | 2Φ16 | 0.25 | 2Φ12 | 1.01 | Φ10@15 | 4Φ8@10 | 4Φ12 | 25 | 0.56 |
| S8 | 32.3 | 401.9 | 265 | 33 | 2Φ20 | 0.36 | 2Φ16 | 1.58 | Φ10@15 | 4Φ8@10 | ----- | 25 | 0.64 |
| SH1 | 64.6 | 398.0 | 269 | 30 | 2Φ12 | 0.10 | 2Φ10 | 0.56 | Φ10@15 | ----- | ----- | 25 | 0.70 |
| SH2 | 52.7 | 400.0 | 261 | 29 | 2Φ28 | 0.66 | 2Φ8 | 3.15 | Φ10@13 | ----- | ----- | 25 | 0.08 |
| SH3 | 73.5 | 400.0 | 261 | 35 | 2Φ28 | 0.41 | 2Φ20 | 3.15 | Φ10@12 | ----- | ----- | 25 | 0.51 |
| SH4 | 61.1 | 370.0 | 263 | 35 | 2Φ25 | 0.37 | 2Φ20 | 2.49 | Φ10@6.5 | ----- | ----- | 25 | 0.64 |

SH4. The studied parameters include concrete strength and the flexural tensile and compressive reinforcement ratio $\rho$ and $\rho'$.

## 2.2 Materials and mix design of SCCs

Locally available deformed bars were used as flexural and shear reinforcement rebar. The steel yield stress obtained from tension tests are listed in Table 1. The concrete mixtures for the specimens were mixed in 200 litter capacity batch mixer. The mix design of concrete used for NSSCC and HSSCC members are shown in Table 2. The obtained range of results in fresh phase presented in Table 3, it was found that the SCCs were consolidate exceptionally well under its own weight. The compressive concrete strength $f_c'$ for each beam is shown in Table 1. All beams and control specimens were cast and cured under similar conditions. The beams and specimens were kept covered under polyethylene sheets for 28 days.

The mix properties of SCCs and the range of fresh properties obtained are summarized in Tables 2 and 3 respectively.

Table 2 Mix design of NSSCC and HSSCC (1 m$^3$)

| Concrete type | W/P | Cement (kg) | Gravel (kg) | Sand (kg) | Limestone powder (kg) | Micro silica (kg) | PCE (Lit) |
|---|---|---|---|---|---|---|---|
| S | 0.39 | 270 | 750 | 870 | 225 | 30 | 4 |
| SH | 0.31 | 450 | 800 | 830 | 100 | 50 | 5 |

Table 3 Fresh properties of SCCs

| Concrete type | V-funnel Flow time (s) | L-box ($h_2/h_1$) | Slump flow Diameter (mm) |
|---|---|---|---|
| S | 5 | 0.80-0.82 | 70-72 |
| SH | 7.2-9.5 | 0.78-0.85 | 680-720 |

Fig. 2 Extent of crushing at ultimate and buckling of compression steel after failure

## 2.3 Casting, instrumentation and testing of members

Electrical resistance disposable strain gauges, manufactured by TML Measurements Group (Japan), were pasted on the internal reinforcing bars at different locations. The demec points and electrical gauges were also attached along the height of members to measure the concrete strains; these values can be used to find out the strain distribution and the moving neutral axis depth of the members tested. All connections were loaded in three-point bending to failure with a clear span of 2.7 m, and loading points were located on top surface of stub at mid-span location (Fig. 1). The load was applied step-by-step up to failure in a load control manner of test beams. The experimental values of steel tensile and compressive strain ($\varepsilon_s$, $\varepsilon_s'$), the extreme layer of concrete compressive strain ($\varepsilon_c$), and vertical deflections were also measured (using LVDTs) during the test. The strain gauges, LVDTs, and the load cell were connected through a data acquisition system to a computer and the data was recorded and stored in the computer (Fig. 2). The crack widths was measured by crack detection microscope with an accuracy of 0.02 mm.

The experimental program was conducted by testing of 12 simulated beam-column connections in reinforced NSSCC and HSSCC. The variables studied included concrete strength, tensile and compressive steel ratio, $\rho$, $\rho'$ and the ratio of $\rho'/\rho$. As yet there is no any available design code for reinforced SCC; the maximum and minimum reinforcement ratios are in accordance with the provision of the ACI-05 (2005) for conventional RC and only net tensile failure connections were included. The details of specimens tested in the research program are presented in Table 1.

The rebar were tested in tension and an average yield stress, ($f_y$) values of 400 MPa was reported (Mohamadi 2007).

## 2.4 Test procedure

The specimens were tested under simply supported conditions and were subjected under three-point loading, as shown in Fig. 1(b). The crack widths was measured by crack detection microscope with an accuracy of 0.02 mm, and deflections were measured at different points as shown in Fig. 2, but only the results of the member midspan deflection are reported here. Strain in the tension ($\varepsilon_s$)

Fig. 3 Details of loading system and measurement schemes

and compression ($\varepsilon_s'$) steel were measured by electrical strain gauges. In addition, concrete strains ($\varepsilon_c$) using demec gauges fixed at different sections were measured (see Fig. 1), but again the results of the member midspan concrete strain are reported.

Increments of load were applied gradually. The first few load increments were between 500-1000 kg and after the occurrence of a visible crack width of approximately 0.01 mm, then the load increments was increased. Again near the steel yield strain, the load increments were reduced for a better judgment of the behavior of the steel horizontal yield plateau.

Each increment of load was applied over a time period of 1 minute and held constant for an approximately additional 15 minute. The cracks were marked and the concrete strain measured during the 15 minute interval between load applications. At the end of each load increment, observations, measurements and cracks development and propagation on the beam surfaces were recorded (Fig. 3). A complete test ideally required twenty increments and took about 5-6 hours.

## 3. Experimental results

All members tested in flexure exhibited vertical flexural cracks in the maximum moment region before final failure of the members due to crushing of concrete. Fig. 4 shows the crack propagation and development pattern under the load for some typical member.

The measured values of steel tensile strain ($\varepsilon_s$) and concrete compressive strain ($\varepsilon_c$) were then converted to stresses at three different levels of flexural crack width (i.e., 0.1, 0.2, 0.3 mm) and shown in Table 4. The ratios of $f_s/f_y$ and $f_c/f_c'$ are also presented in Table 4.

For conventional normal strength concrete (NSC), the analysis of section may be considered as linear, when ratios of $f_c/f_c'$ and $f_s/f_y$ does not exceed the values of 0.5 and 0.62 respectively. No suggestion exists in literature for limiting values of $f_c/f_c'$ and $f_s/f_y$ for conventional high strength concrete (HSC) flexural members, the values suggested for NSC will be assumed for SCCs of this study. Based on this assumption, it can be seen that irrespective of the amount of $\rho, \rho', f_y, f_c'$, for all tested members, these two coefficients are equal to or less than 0.5 and 0.62 for permissible crack widths of 0.1 and 0.2 mm respectively (except the connections S5, S6, SH2, SH3, SH4). However,
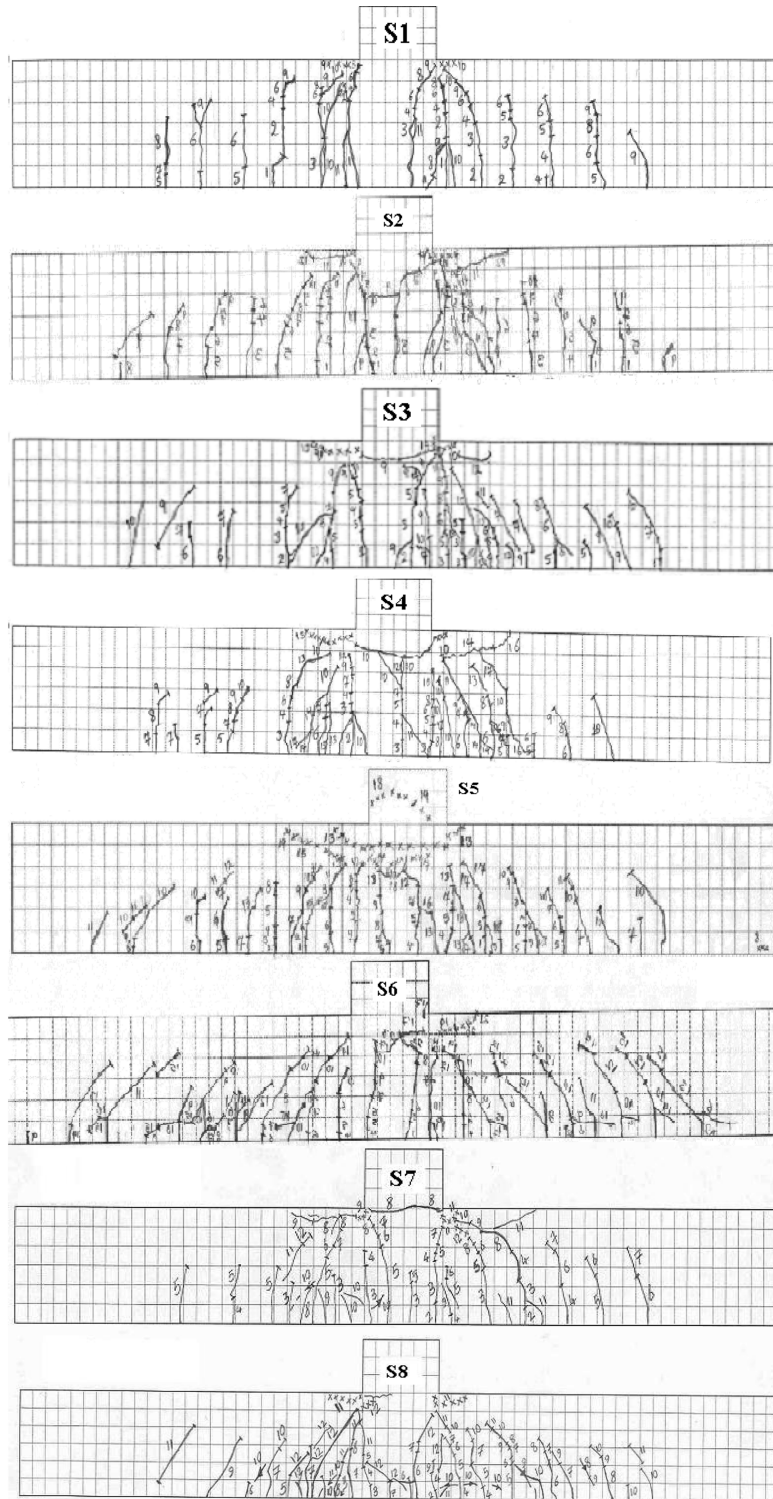
Fig. 4(a) Cracks development pattern of reinforced SCCs members under load (S series)
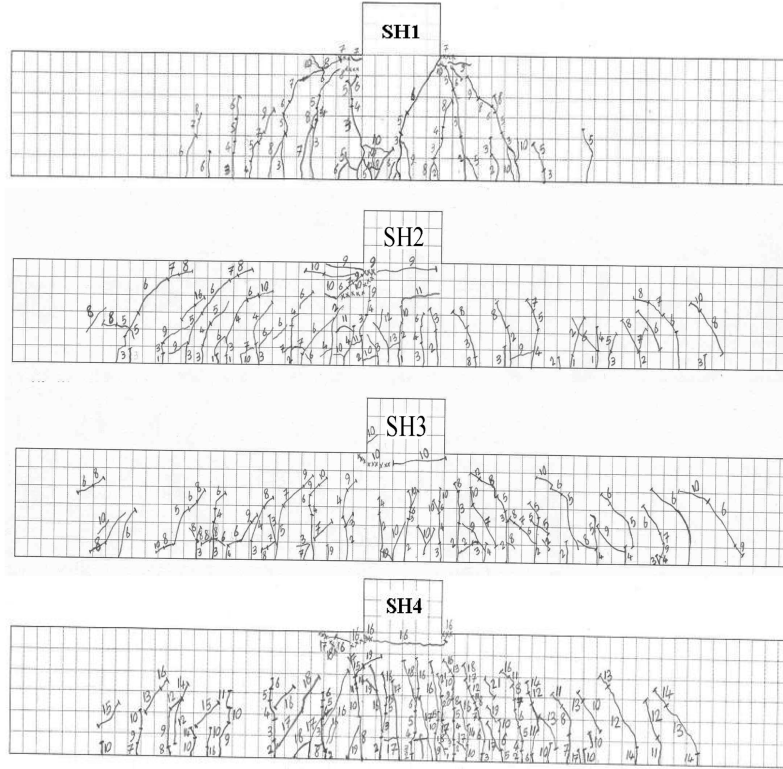
Fig. 4(b) Cracks development pattern of reinforced SCCs members under load (HS series)

a close observation results of Table 4 indicate that, often the coefficient $f_s/f_y$ even for a crack width of 0.3 mm is much lower than 0.62 (except the members S8, SH3). It seems it can be concluded that, for such non vibrating concrete, the bound between reinforcing steels and surrounding concrete is excellent.

The flexural crack width of SCCs specimens was also investigated and the results are shown in Table 5. The applicability of crack width Eqs. (2), (3) and (4) for conventional normal strength concrete, as per ACI-318 (2005), BS-8110 (1985) and CSA (1994) code, was verified for members tested.

Different parameters of Eqs. (2), (3) and (4) were either calculated or measured for crack widths levels of 0.1, 0.2, 0.3 mm for (ACI-318 2005, BS-8110 1985) and the crack width limitation specified in (CSA 1994) in terms of quantity "$Z$" for interior and exterior exposure, and the results are presented in Table 5.

$$\omega_{cr} = C\beta_h f_s \sqrt[3]{d_c A} \tag{2}$$

$$\omega_{cr} = \frac{4.5 a_{cr} \varepsilon_m}{1 + 2.5\left(\dfrac{a_{cr} - c}{h - x}\right)} \tag{3}$$

$$Z = f_s (d_c A)^{1/3} \tag{4}$$

Table 4 Experimental values of concrete and steel for different permissible flexural crack width for specimens (at 15 cm from mid span)

| Specimen | $w_{cr}$ (mm) | Tensile Steel | | | Concrete | | | Compressive Steel | |
|---|---|---|---|---|---|---|---|---|---|
| | | $\varepsilon_s$ | $f_s$ [MPa] | $f_s/f_y$ | $\varepsilon_c$ | $f_c$ [MPa] | $f_c/f_c'$ [MPa] | $\varepsilon_s'$ | $f_s'$ [MPa] |
| SH1 | 0.1 | 0.00069 | 138.69 | 0.347 | 0.00027 | 9.07 | 0.14 | 116 | 23.20 |
| | 0.2 | 0.00076 | 152.76 | 0.382 | 0.00029 | 9.74 | 0.15 | 134 | 26.80 |
| | 0.3 | 0.00104 | 209.04 | 0.523 | 0.00045 | 15.11 | 0.23 | 106 | 21.20 |
| SH2 | 0.1 | 0.00048 | 96.48 | 0.241 | 0.00050 | 15.50 | 0.29 | 420 | 84.00 |
| | 0.2 | 0.00085 | 170.85 | 0.427 | 0.00118 | 36.58 | 0.69 | 660 | 132.00 |
| | 0.3 | 0.00115 | 231.15 | 0.578 | 0.00133 | 41.23 | 0.78 | 880 | 176.00 |
| SH3 | 0.1 | 0.00086 | 172.86 | 0.432 | 0.00135 | 47.74 | 0.65 | 250 | 50.00 |
| | 0.2 | 0.00118 | 237.18 | 0.593 | 0.00169 | 59.76 | 0.81 | 410 | 82.00 |
| | 0.3 | 0.00168 | 337.68 | 0.844 | 0.00217 | 76.74 | 1.04 | 500 | 100.00 |
| SH4 | 0.1 | 0.00063 | 126.63 | 0.317 | 0.00087 | 28.58 | 0.47 | 125 | 25.00 |
| | 0.2 | 0.00069 | 138.69 | 0.347 | 0.00097 | 31.87 | 0.52 | 145 | 29.00 |
| | 0.3 | 0.00094 | 188.94 | 0.472 | 0.00127 | 41.72 | 0.68 | 190 | 38.00 |
| S1 | 0.1 | 0.00046 | 92.46 | 0.231 | 0.00008 | 2.10 | 0.07 | 400 | 80.00 |
| | 0.2 | 0.00074 | 148.74 | 0.372 | 0.00012 | 3.15 | 0.10 | 740 | 148.00 |
| | 0.3 | 0.00096 | 192.96 | 0.482 | 0.00022 | 5.77 | 0.19 | 1000 | 200.00 |
| S2 | 0.1 | 0.00036 | 72.36 | 0.181 | 0.00021 | 5.46 | 0.18 | 330 | 66.00 |
| | 0.2 | 0.00085 | 170.85 | 0.427 | 0.00039 | 10.15 | 0.34 | 860 | 172.00 |
| | 0.3 | 0.00123 | 247.23 | 0.618 | 0.00075 | 19.52 | 0.66 | 1230 | 246.00 |
| S3 | 0.1 | 0.00051 | 102.51 | 0.256 | 0.00026 | 6.57 | 0.23 | 540 | 108.00 |
| | 0.2 | 0.00074 | 148.74 | 0.372 | 0.00043 | 10.86 | 0.39 | 700 | 140.00 |
| | 0.3 | 0.00083 | 166.83 | 0.411 | 0.00058 | 14.65 | 0.52 | 830 | 166.00 |
| S4 | 0.1 | 0.00053 | 106.53 | 0.266 | 0.00048 | 12.72 | 0.41 | 520 | 104.00 |
| | 0.2 | 0.00094 | 188.94 | 0.472 | 0.00057 | 15.11 | 0.49 | 940 | 188.00 |
| | 0.3 | 0.00118 | 237.18 | 0.593 | 0.00071 | 18.82 | 0.61 | 1150 | 230.00 |
| S5 | 0.1 | 0.00048 | 96.48 | 0.241 | 0.00093 | 25.39 | 0.78 | 488 | 97.60 |
| | 0.2 | 0.00087 | 174.87 | 0.437 | 0.00133 | 36.32 | 1.11 | 871 | 174.20 |
| | 0.3 | 0.00122 | 245.22 | 0.613 | 0.00174 | 47.51 | 1.45 | 1200 | 240.00 |
| S6 | 0.1 | 0.00026 | 52.26 | 0.132 | 0.00042 | 11.11 | 0.36 | 244 | 48.80 |
| | 0.2 | 0.00057 | 114.57 | 0.286 | 0.00103 | 27.25 | 0.89 | 572 | 114.40 |
| | 0.3 | 0.00112 | 225.12 | 0.563 | 0.00193 | 51.06 | 1.66 | 1104 | 220.80 |
| S7 | 0.1 | 0.00045 | 90.45 | 0.226 | 0.00021 | 5.27 | 0.19 | 100 | 20.00 |
| | 0.2 | 0.00069 | 138.69 | 0.347 | 0.00025 | 6.27 | 0.23 | 150 | 30.00 |
| | 0.3 | 0.00111 | 223.11 | 0.558 | 0.00068 | 17.06 | 0.62 | 200 | 40.00 |
| S8 | 0.1 | 0.00051 | 102.51 | 0.256 | 0.00036 | 9.77 | 0.30 | 125 | 25.00 |
| | 0.2 | 0.00085 | 170.85 | 0.427 | 0.00055 | 14.93 | 0.46 | 183 | 36.60 |
| | 0.3 | 0.00126 | 253.26 | 0.633 | 0.00089 | 24.15 | 0.75 | 237 | 47.40 |

Table 5(a) Experimental and calculated crack width based on BS 8110

| | | | | | | | |
|---|---|---|---|---|---|---|---|
| | | | $(\omega_{cr})_{th}$ Based on Eq. (3) | | | | |
| | | | [*]$(\omega_{cr})$ = 0.1 (mm) | | | | |
| Member No. | $a_{cr}$ (mm) | $(X)_{exp}$ (mm) | $(f_s)_{exp}$ (MPa) | $\varepsilon_1 \times 10^{-3}$ | $\varepsilon_m \times 10^{-3}$ | $(\omega_{cr})_{th}$ (mm) | $((\omega_{cr})_{th}/(\omega_{cr})_{exp})$ |
| SH1 | 37.8 | 64.2 | 138.69 | 0.80 | 0.50 | 0.07 | 0.75 |
| SH2 | 41.2 | 109.7 | 96.48 | 0.61 | 0.56 | 0.09 | 0.85 |
| SH3 | 41.2 | 160.5 | 172.86 | 1.20 | 1.16 | 0.17 | 1.67 |
| SH4 | 39.8 | 142.4 | 126.63 | 0.83 | 0.77 | 0.11 | 1.12 |
| S1 | 47.3 | 20.8 | 92.46 | 0.53 | 0.02 | 0.00 | 0.04 |
| S2 | 48.6 | 170.6 | 72.36 | 0.52 | 0.41 | 0.07 | 0.67 |
| S3 | 49.4 | 93.7 | 102.51 | 0.64 | 0.54 | 0.10 | 0.99 |
| S4 | 49.4 | 49.3 | 106.53 | 0.64 | 0.52 | 0.10 | 0.99 |
| S5 | 48.3 | 170.0 | 96.48 | 0.72 | 0.67 | 0.11 | 1.09 |
| S6 | 48.2 | 171.6 | 52.26 | 0.40 | 0.36 | 0.06 | 0.57 |
| S7 | 38.7 | 54.4 | 90.45 | 0.52 | 0.35 | 0.05 | 0.53 |
| S8 | 39.5 | 75.1 | 102.51 | 0.61 | 0.50 | 0.08 | 0.77 |
| | | | [**]$(\omega_{cr})$ = 0.2 (mm) | | | | |
| Beam No. | $a_{cr}$ (mm) | $(X)_{exp}$ (mm) | $(f_s)_{exp}$ (MPa) | $\varepsilon_1 \times 10^{-3}$ | $\varepsilon_m \times 10^{-3}$ | $(\omega_{cr})_{th}$ (mm) | $((\omega_{cr})_{th}/(\omega_{cr})_{exp})$ |
| SH1 | 37.8 | 65.6 | 152.76 | 0.88 | 0.58 | 0.09 | 0.44 |
| SH2 | 41.2 | 132.0 | 170.85 | 1.11 | 1.07 | 0.16 | 0.80 |
| SH3 | 41.2 | 157.7 | 237.18 | 1.63 | 1.59 | 0.23 | 1.15 |
| SH4 | 39.8 | 140.0 | 138.69 | 0.90 | 0.85 | 0.12 | 0.61 |
| S1 | 47.3 | 35.5 | 148.74 | 0.86 | 0.38 | 0.07 | 0.35 |
| S2 | 48.6 | 72.2 | 170.85 | 1.04 | 0.86 | 0.16 | 0.80 |
| S3 | 49.4 | 98.7 | 148.74 | 0.94 | 0.84 | 0.15 | 0.77 |
| S4 | 49.4 | 76.3 | 188.94 | 1.16 | 1.05 | 0.20 | 0.98 |
| S5 | 48.3 | 162.0 | 174.87 | 1.27 | 1.22 | 0.20 | 1.00 |
| S6 | 48.2 | 156.7 | 114.57 | 0.83 | 0.78 | 0.13 | 0.65 |
| S7 | 38.7 | 71.4 | 138.69 | 0.81 | 0.64 | 0.10 | 0.49 |
| S8 | 39.5 | 99.0 | 170.85 | 1.03 | 0.94 | 0.14 | 0.71 |
| | | | [***]$(\omega_{cr})$ = 0.3 (mm) | | | | |
| Beam No. | $a_{cr}$ (mm) | $(X)_{exp}$ (mm) | $(f_s)_{exp}$ (MPa) | $\varepsilon_1 \times 10^{-3}$ | $\varepsilon_m \times 10^{-3}$ | $(\omega_{cr})_{th}$ (mm) | $((\omega_{cr})_{th}/(\omega_{cr})_{exp})$ |
| SH1 | 37.8 | 73.5 | 209.04 | 1.21 | 0.92 | 0.14 | 0.46 |
| SH2 | 41.2 | 134.6 | 231.15 | 1.51 | 1.47 | 0.22 | 0.73 |
| SH3 | 41.2 | 154.9 | 337.68 | 2.31 | 2.27 | 0.33 | 1.10 |
| SH4 | 39.8 | 135.0 | 188.94 | 1.22 | 1.16 | 0.17 | 0.56 |
| S1 | 47.3 | 42.7 | 192.96 | 1.13 | 0.65 | 0.12 | 0.40 |
| S2 | 48.6 | 77.1 | 247.23 | 1.51 | 1.34 | 0.25 | 0.82 |
| S3 | 49.4 | 101.0 | 166.83 | 1.06 | 0.96 | 0.17 | 0.58 |
| S4 | 49.4 | 94.0 | 237.18 | 1.49 | 1.39 | 0.25 | 0.85 |
| S5 | 48.3 | 158.0 | 245.22 | 1.76 | 1.71 | 0.28 | 0.94 |
| S6 | 48.2 | 156.3 | 225.12 | 1.62 | 1.58 | 0.26 | 0.87 |
| S7 | 38.7 | 93.8 | 223.11 | 1.33 | 1.18 | 0.18 | 0.58 |
| S8 | 39.5 | 108.9 | 253.26 | 1.55 | 1.46 | 0.22 | 0.73 |

[*]$\omega_{cr}$ permissible = $(\omega_{cr})_{exp}$ = 0.1 (mm), [**]$\omega_{cr}$ permissible = $(\omega_{cr})_{exp}$ = 0.2 (mm), [***]$\omega_{cr}$ permissible = $(\omega_{cr})_{exp}$ = 0.3 (mm)

Table 5(b) Experimental and calculated crack width based on ACI 318-04

| | | | | $(\omega_{cr})_{th}$ Based on Eq. (2) | |
|---|---|---|---|---|---|
| | | | $^*(\omega_{cr}) = 0.1$ (mm) | | |
| Member No. | $\beta_h$ | $d_c$ (mm) | $A$ (mm) | $(\omega_{cr})_{th}$ (mm) | $((\omega_{cr})_{th}/ (\omega_{cr})_{exp})$ |
| SH1 | 1.15 | 31 | 4650 | 0.09 | 0.90 |
| SH2 | 1.26 | 39 | 5850 | 0.08 | 0.80 |
| SH3 | 1.39 | 39 | 5850 | 0.16 | 1.58 |
| SH4 | 1.31 | 37 | 5550 | 0.11 | 1.05 |
| S1 | 1.15 | 37 | 5550 | 0.07 | 0.68 |
| S2 | 1.45 | 40 | 6000 | 0.07 | 0.70 |
| S3 | 1.26 | 42 | 6300 | 0.09 | 0.89 |
| S4 | 1.20 | 42 | 6300 | 0.09 | 0.89 |
| S5 | 1.49 | 43 | 6450 | 0.10 | 1.02 |
| S6 | 1.52 | 44 | 6600 | 0.06 | 0.57 |
| S7 | 1.16 | 33 | 4950 | 0.06 | 0.62 |
| S8 | 1.18 | 35 | 5250 | 0.07 | 0.75 |
| | | | $^{**}(\omega_{cr}) = 0.2$ (mm) | | |
| SH1 | 1.15 | 31 | 4650 | 0.10 | 0.50 |
| SH2 | 1.30 | 39 | 5850 | 0.15 | 0.73 |
| SH3 | 1.38 | 39 | 5850 | 0.22 | 1.08 |
| SH4 | 1.30 | 37 | 5550 | 0.11 | 0.57 |
| S1 | 1.16 | 37 | 5550 | 0.11 | 0.55 |
| S2 | 1.21 | 40 | 6000 | 0.14 | 0.70 |
| S3 | 1.26 | 42 | 6300 | 0.13 | 0.65 |
| S4 | 1.23 | 42 | 6300 | 0.16 | 0.81 |
| S5 | 1.45 | 43 | 6450 | 0.18 | 0.89 |
| S6 | 1.44 | 44 | 6600 | 0.12 | 0.59 |
| S7 | 1.17 | 33 | 4950 | 0.10 | 0.48 |
| S8 | 1.21 | 35 | 5250 | 0.13 | 0.64 |
| | | | $^{***}(\omega_{cr}) = 0.3$ (mm) | | |
| SH1 | 1.16 | 31 | 4650 | 0.14 | 0.46 |
| SH2 | 1.31 | 39 | 5850 | 0.20 | 0.67 |
| SH3 | 1.37 | 39 | 5850 | 0.30 | 1.02 |
| SH4 | 1.29 | 37 | 5550 | 0.16 | 0.52 |
| S1 | 1.17 | 37 | 5550 | 0.14 | 0.48 |
| S2 | 1.22 | 40 | 6000 | 0.20 | 0.67 |
| S3 | 1.27 | 42 | 6300 | 0.15 | 0.49 |
| S4 | 1.26 | 42 | 6300 | 0.21 | 0.69 |
| S5 | 1.43 | 43 | 6450 | 0.25 | 0.83 |
| S6 | 1.44 | 44 | 6600 | 0.23 | 0.77 |
| S7 | 1.19 | 33 | 4950 | 0.16 | 0.52 |
| S8 | 1.22 | 35 | 5250 | 0.19 | 0.63 |

$^*\omega_{cr}$ permissible $= (\omega_{cr})_{exp} = 0.1$ (mm), $^{**}\omega_{cr}$ permissible $= (\omega_{cr})_{exp} = 0.2$ (mm), $^{***}\omega_{cr}$ permissible $= (\omega_{cr})_{exp} = 0.3$ (mm)

Table 5(c) Experimental and calculated crack width based on CSA

| Member No. | Interior exposure ($\omega_{cr}$ = 0.33 mm) | | | Interior exposure ($\omega_{cr}$ = 0.40 mm) | | | $w_{(cr)}$ (0.6$f_y$) |
|---|---|---|---|---|---|---|---|
| | $(f_s)_{exp}$ (MPa) | Z (N/mm) | Z/25000 | $(f_s)_{exp}$ (MPa) | Z (N/mm) | Z/30000 | |
| S1 | 220 | 11535 | 0.46 | 552 | 28943 | 0.96 | 0.33 |
| S2 | 276 | 16865 | 0.67 | 316 | 19309 | 0.64 | 0.27 |
| S3 | 170 | 10388 | 0.42 | 200 | 12221 | 0.41 | 0.41 |
| S4 | 252 | 14867 | 0.59 | 294 | 17345 | 0.58 | 0.31 |
| S5 | 256 | 15103 | 0.60 | 280 | 16519 | 0.55 | 0.26 |
| S6 | 238 | 14766 | 0.59 | 252 | 15648 | 0.52 | 0.39 |
| S7 | 264 | 16949 | 0.68 | 308 | 19773 | 0.66 | 0.28 |
| S8 | 270 | 17334 | 0.69 | 294 | 18875 | 0.63 | 0.28 |
| SH1 | 226 | 14738 | 0.59 | 278 | 18130 | 0.60 | 0.34 |
| SH2 | 262 | 17350 | 0.69 | 282 | 18674 | 0.62 | 0.31 |
| SH3 | 356 | 19461 | 0.78 | 414 | 22631 | 0.75 | 0.21 |
| SH4 | 220 | 12507 | 0.50 | 260 | 14781 | 0.49 | 0.34 |

$Z \leq 30000$ N/mm for interior exposure (i.e., $\omega_{cr}$ = 0.40 mm) and 25000 N/mm for exterior exposure (i.e., $\omega_{cr}$ = 0.33 mm)
where

$$C = 108 \times 10^{-7} \text{ (mm}^2\text{/N)}, \quad \beta_h = \frac{h_2}{h_1}$$

$$A = \frac{2yb_w}{Number\ of\ tensile\ bar}, \quad \varepsilon_m = \varepsilon_1 - \frac{b_t(h-x)(a'-x)}{3E_sA_s(d-x)}, \quad \varepsilon_1 = \frac{h-x}{d-x}\frac{f_s}{E_s}$$

The parameters of Eqs. (2) and (3) are shown in Figs. 5 and 6 respectively.

It can be seen from Table 5 that for a crack width 0.1 mm, the measured experimental crack width $(\omega_{cr})_{exp}$ were very close to the predictions by Eqs. (3) and (2) which are suggested by British standard and ACI code respectively (except member, SH3).

Considering crack width of 0.2 mm; comparison of the experimental results indicated that, the predictions of Eq. (3) were close to the values of $(\omega_{cr})_{exp}$ for connections (S4, S5, SH3), and for other 9 members the values of $(\omega_{cr})_{th}$ were smaller than $(\omega_{cr})_{exp}$. For Eq. (2) the calculated values of $(\omega_{cr})_{th}$ are smaller than the measured values of $(\omega_{cr})_{exp}$ (except SH3).

Assuming crack width 0.3 mm; again, the obtained theoretical values are smaller than experimental values as estimated after Eqs. (2) and (3), respectively.

In general, for almost all HSSCC members tested at the three levels of crack width (0.1, 0.2, 0.3 mm); the use of ACI Eq. (2) led to predict 33% of the results conservative (the ratio of (($\omega_{cr})_{th}$/ $(\omega_{cr})_{exp}$) is greater than unity). However, considering Eq. (2) for the same levels of crack widths for NSSCC members, led to predict the unconservative results (the ratio of (($\omega_{cr})_{th}$/$(\omega_{cr})_{exp}$) is smaller than unity (except for S5 for crack width of 0.1 mm)). The results of the BS Eq. (3) were noted to be conservative while compare to the ACI Eq. (2).
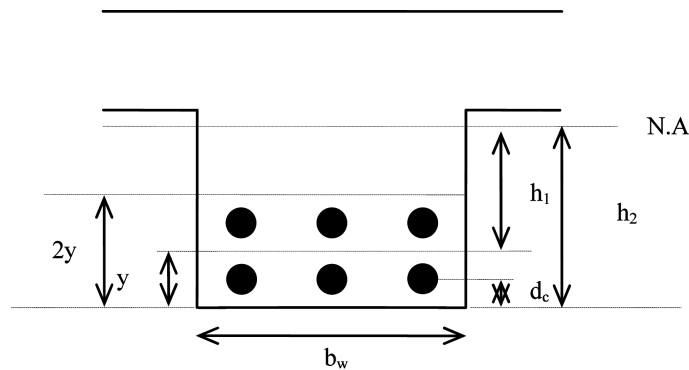
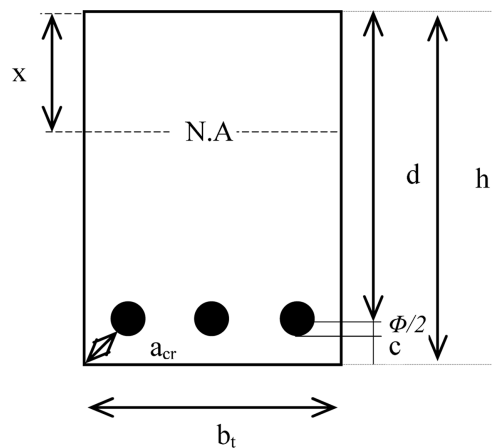Fig. 5 Parameters identification of Eq. (2)



Fig. 6 Parameters identification of Eq. (3)

Two crack width limitation specified in CSA based on Eq. (4), are calculated and their comparison with the experimental results are shown in Table 5(c).

Considering CSA method; the quantity of "Z" for NSC members predicted for both interior and exterior exposure is applicable in SCCs members also. By use of a higher reinforcement ratio, the quantity of "Z" obtained is more conservative, and for the case of a lower reinforcement ratio, the obtained "Z" is closer to limiting values of CSA. It is clear from Table 5(c) that, although for interior exposure of S1 and SH3 members, the tensile steels reached the yield stress, but the crack widths were never increased more than limiting value of 0.4 mm even for the S1 specimen consisting of $\rho_{min}$ value. For crack control, it is a usual practice to limit the value of tensile steel to $0.6f_y$. For this limiting value, the average crack width of tested members is 0.31 mm which is lower than the suggested values for exterior and interior exposure for NSC members.

It seems that, the obtained results are indicating that a very good bond is available between the bars and the surrounding concrete area in both type of SCCs tested specimens.

The load versus deflection relationships for the different reinforcement ratios are shown in Fig. 7. Table 6 presents the experimentally and theoretically (ACI & CSA) obtained cracking and yielding moments for the tested members. The experimental cracking moment, $M_{cr(exp)}$, corresponds to the
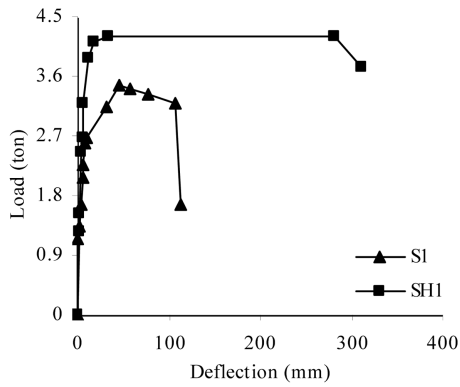
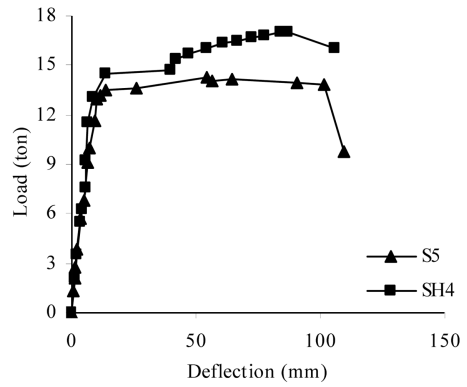Fig. 7(a) Load-deflection curves of tested connections (S1, SH1)



Fig. 7(b) Load-deflection curves of tested connections (S5, SH4)
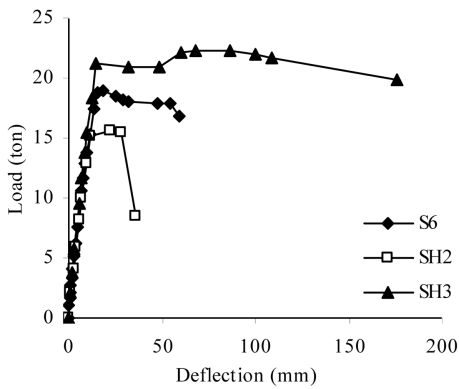


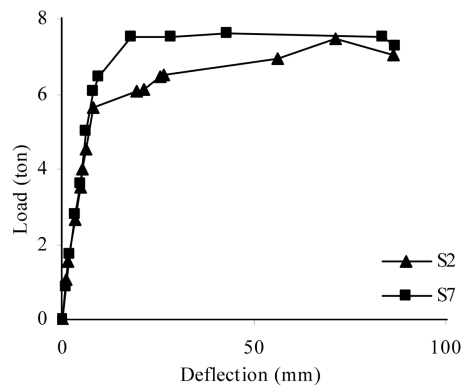Fig. 7(c) Load-deflection curves of tested connections (S6, SH2, SH3)



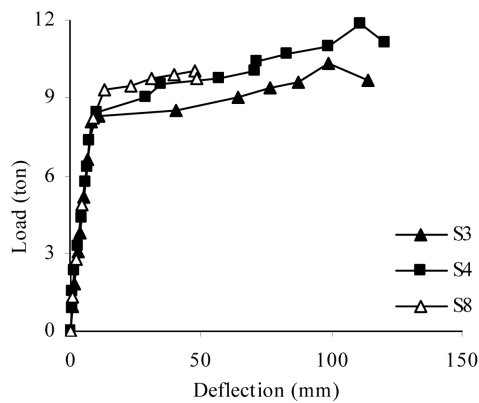Fig. 7(d) Load-deflection curves of tested connections (S2, S7)



Fig. 7(e) Load-deflection curves of tested connections (S3, S4, S8)

Table 6 Experimental and theoretical values of cracking moment of tested members

| Member No. | $M_{cr(exp)}$ ton.m | $M_{y(exp)}$ ton.m | $M_{cr(th-ACI)}$ ton.m | $M_{cr(th-CSA)}$ ton.m | $M_{cr(exp)}$ / $M_{cr(th-ACI)}$ | $M_{cr(exp)}$ / $M_{cr(th-CSA)}$ |
|---|---|---|---|---|---|---|
| SH1 | 0.827 | 2.370 | 1.121 | 1.085 | 0.738 | 0.762 |
| SH2 | 1.151 | 9.072 | 1.013 | 0.981 | 1.136 | 1.173 |
| SH3 | 2.014 | 12.706 | 1.196 | 1.157 | 1.684 | 1.741 |
| SH4 | 0.619 | 8.160 | 1.090 | 1.055 | 0.568 | 0.587 |
| S1 | 0.763 | 1.753 | 0.742 | 0.765 | 1.028 | 0.997 |
| S2 | 0.715 | 3.821 | 0.735 | 0.762 | 0.973 | 0.938 |
| S3 | 1.208 | 5.439 | 0.749 | 0.774 | 1.613 | 1.561 |
| S4 | 1.573 | 5.701 | 0.714 | 0.738 | 2.203 | 2.131 |
| S5 | 0.898 | 8.721 | 0.772 | 0.798 | 1.163 | 1.125 |
| S6 | 2.206 | 11.733 | 0.748 | 0.773 | 2.949 | 2.854 |
| S7 | 0.937 | 3.726 | 0.733 | 0.710 | 1.278 | 1.320 |
| S8 | 0.721 | 5.226 | 0.793 | 0.767 | 0.909 | 0.940 |

moment at which initial slope of the load-deflection curve deviates. The experimental yielding moment, $M_{y(exp)}$, corresponds to the moment at which, yielding flat plateau is observed in the load-deflection curve. A comparison between two Codes (ACI and CSA) for the theoretical values is also shown in this Table. It is obvious that, irrespective of the concrete strength, for the specimens reported, the prediction values of two codes are almost equaled.

In general, for all HSSCC members tested the use of two codes led to predict 50% of the results conservative (the ratio of (the ratio of $M_{cr)th}/(M_{cr})_{exp}$ is greater than unity), and for NSSCC, it led to predict unconservative results for 37.5% and 62.5% of the results (the ratio of $M_{cr)th}/(M_{cr})_{exp}$ is respectively greater and smaller than unity).

## 3.1 Cracking moment

The analytical evaluation of deflection depends greatly on the cracking moment of the members. Cracking moment is usually estimated using the modulus of rupture as

$$M_{cr} = \frac{f_r \cdot I_g}{y_t} \qquad (5)$$

$$f_r = 0.62\sqrt{f_c'} \quad \text{MPa (ACI)} \qquad (6)$$

$$f_r = 0.6\sqrt{f_c'} \quad \text{MP (CSA)} \qquad (7)$$

The experimental cracking moment, $M_{cr(exp)}$, is used to determine the experimental cracking stress, $f_{r(exp)}$. The variation of ratio of $f_{r(exp)}$ and $f_{r(th)}$ as a function of reinforcement ratio is shown in Fig. 8. The figure indicates that, for SCCs, the experimental cracking stresses are close to theoretical values of ACI and less than the values predicted by CSA for lower $\rho$ values. However, for a higher percentages of $\rho$, some irregularities are occurred and therefore more research work is suggested for
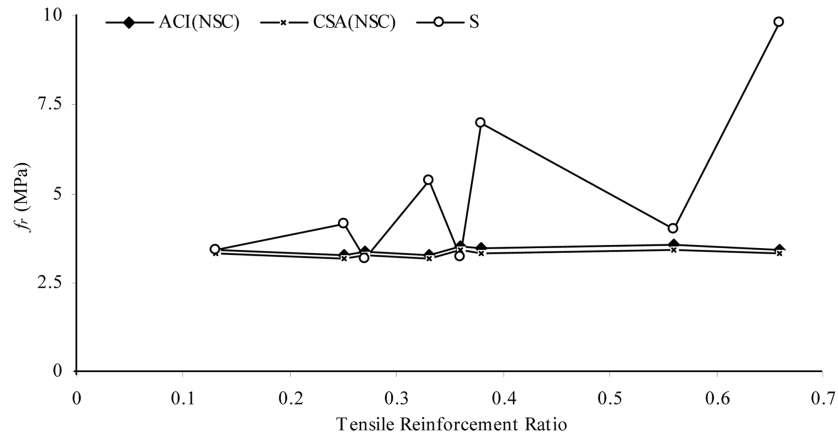
Fig. 8(a) Comparison between experimental and theoretical values of $f_r$ for tested specimens (S series)
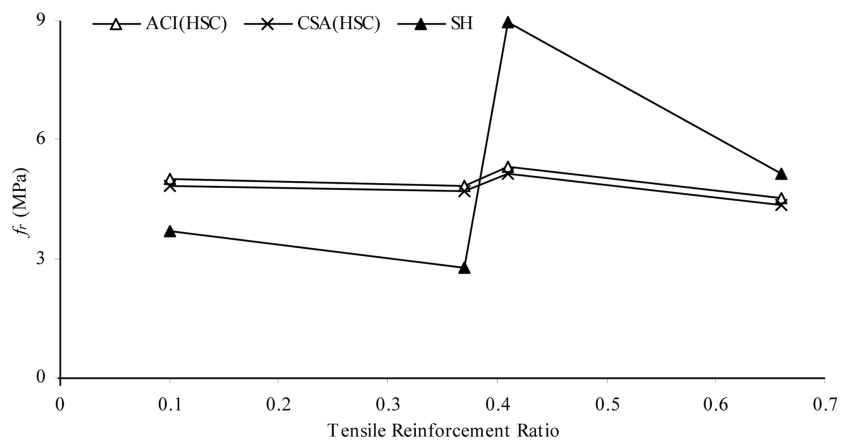


Fig. 8(b) Comparison between experimental and theoretical values of $f_r$ for tested specimens (HS series)

a better understanding effects. It also shows that the suggested values of CSA are always higher than the ACI values.

### 3.2 Neutral axis depth

The experimental variation of depth of the neutral axis, N.A., in the maximum moment section at the yield and ultimate load is shown in Fig. 9 and Table 7. This N.A. depth is obtained from the strain distribution, which was measured experimentally in the compression steel and concrete and the tension reinforcement. The figure shows that the depth of N.A. usually does not vary between cracking and yielding levels. It is clear from the Fig. 9 that, by increasing the amount of $\rho$, the N.A. depth is increased for yield condition.
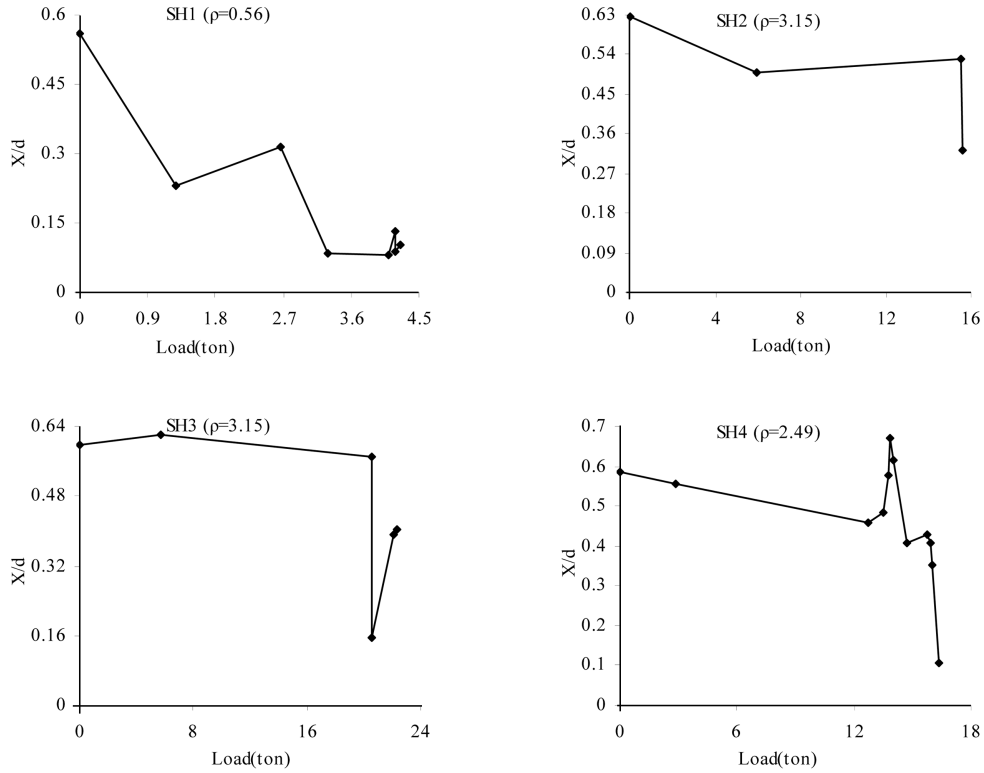
Fig. 9(a) Movement of neutral axis under service load increments (HS series)

## 3.3 Cracked moment of inertia

The calculation of deflection depends basically on the cracked moment of inertia, $I_{cr}$. The experimental cracked moment of inertia based on the elastic deformation theory is obtained by considering

$$i_{cr(\exp1)} = \frac{P_y \cdot l^3}{48 E_c \Delta_{\exp}} \tag{8}$$

$i_{cr}$ can also be defined as the slope of the line connecting the origin and point of initial yielding of tensile reinforcement in moment curvature curve (Ghali 1993, MacGregor and Wight 2005). This is given as

$$i_{cr(\exp2)} = \frac{M_y}{E_c \cdot \phi_y} \tag{9}$$

Where

$$\phi_y = \frac{\varepsilon_{cy} + \varepsilon_{sy}}{d} = \frac{\varepsilon_{cy}}{x}$$

The difference in values of $I_{cr(\exp1)}$ and $I_{cr(\exp2)}$ is expected due to the great variation in curvature
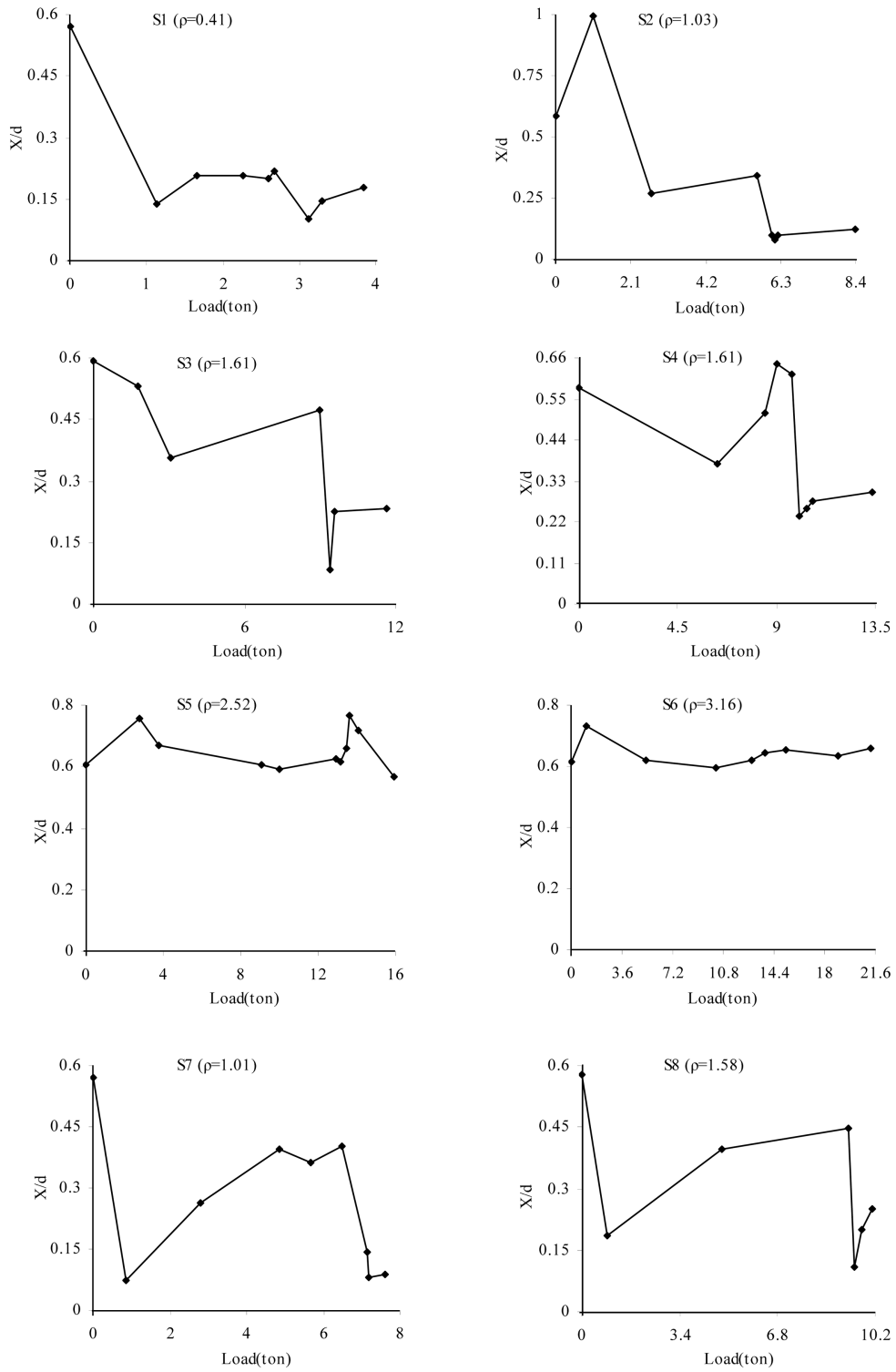
Fig. 9(b) Movement of neutral axis under service load increments (S series)

Table 7 Yield and ultimate loads and the ratio of $X_y/d$ and $X_u/d$ for test members

| Member No. | SH1 | SH2 | SH3 | SH4 | S1 | S2 | S3 | S4 | S5 | S6 | S7 | S8 |
|---|---|---|---|---|---|---|---|---|---|---|---|---|
| $P_u$ | 4.06 | 15.52 | 22.34 | 16.98 | 3.84 | 8.39 | 11.62 | 13.34 | 15.96 | 21.28 | 7.53 | 10.07 |
| $X_u/d$ | 0.083 | 0.045 | 0.403 | 0.106 | 0.179 | 0.123 | 0.231 | 0.301 | 0.566 | 0.661 | 0.087 | 0.246 |
| $P_y$ | 3.95 | 15.12 | 21.18 | 13.61 | 2.92 | 6.37 | 9.07 | 9.50 | 14.54 | 19.56 | 6.21 | 8.71 |
| $X_y/d$ | 0.081 | 0.530 | 0.258 | 0.539 | 0.156 | 0.101 | 0.398 | 0.629 | 0.683 | 0.636 | 0.392 | 0.441 |

distribution along the member especially due to the peaks in curvature at the cracks location.

The traditional theoretical definition of $I_{cr}$ based on the cracked transformed section for conventional reinforced concrete members can be given as:

*Beams with doubly reinforcement*

$$\frac{bx^2}{2} + (A_s + A_s')nx - (A_s d + A_s' d')n - A_s'(x - d') = 0 \tag{10}$$

$$I_{cr} = \frac{bx^3}{3} + nA_s(d-x)^2 + (n-1)A_s'(x-d')^2 \tag{11}$$

where $n = E_s/E_c$ and $E_c = 3200\sqrt{f_c'} + 6900$ (MPa)

Note: In Eqs. (10) and (11) the term $A_s'$ and $d'$ will be ignored when $\rho'$ is not available.

The theoretical and experimental cracked moment of inertia of mentioned equations of conventional reinforced concretes are applied for SCCs and the results are presented in Table 8. It is clear that, for all cases, the values of $I_{cr(exp)}$ are lower than the values of $I_{cr(th)}$, and the values of $I_{cr(exp1)}$ are closer to the $I_{cr(th)}$ and higher than the values of $I_{cr(exp2)}$, except the specimens S4, S6, SH2. Also, the graphical presentation of the values of $I_{cr}/I_g$ for both theoretical and experimental versus $\rho/\rho_b$ are shown in Fig. 10. Referring to Fig. 10, a general conclusion is that, by increasing the

Table 8 Theoretical and experimental cracked moment of inertia

| Member No. | $I_{cr(th)} \times 10^6$ (mm$^4$) | $I_{cr(exp1)} \times 10^6$ (mm$^4$) | $I_{cr(exp2)} \times 10^6$ (mm$^4$) | $I_{cr(th)}/I_{cr(exp1)}$ | $I_{cr(th)}/I_{cr(exp2)}$ |
|---|---|---|---|---|---|
| S1 | 60.62 | 46.32 | 33.12 | 1.31 | 1.83 |
| S2 | 128.93 | 108.79 | 100.03 | 1.19 | 1.29 |
| S3 | 184.01 | 164.08 | 157.98 | 1.12 | 1.16 |
| S4 | 182.23 | 129.58 | 139.45 | 1.41 | 1.31 |
| S5 | 237.93 | 169.60 | 157.88 | 1.40 | 1.51 |
| S6 | 284.30 | 185.48 | 201.30 | 1.53 | 1.41 |
| S7 | 141.39 | 119.42 | 136.51 | 1.18 | 1.04 |
| S8 | 186.42 | 124.16 | 176.76 | 1.50 | 1.05 |
| SH1 | 72.10 | 60.67 | 54.33 | 1.19 | 1.33 |
| SH2 | 253.59 | 179.72 | 225.43 | 1.41 | 1.12 |
| SH3 | 247.06 | 166.56 | 145.22 | 1.48 | 1.70 |
| SH4 | 227.39 | 166.43 | 120.93 | 1.37 | 1.88 |
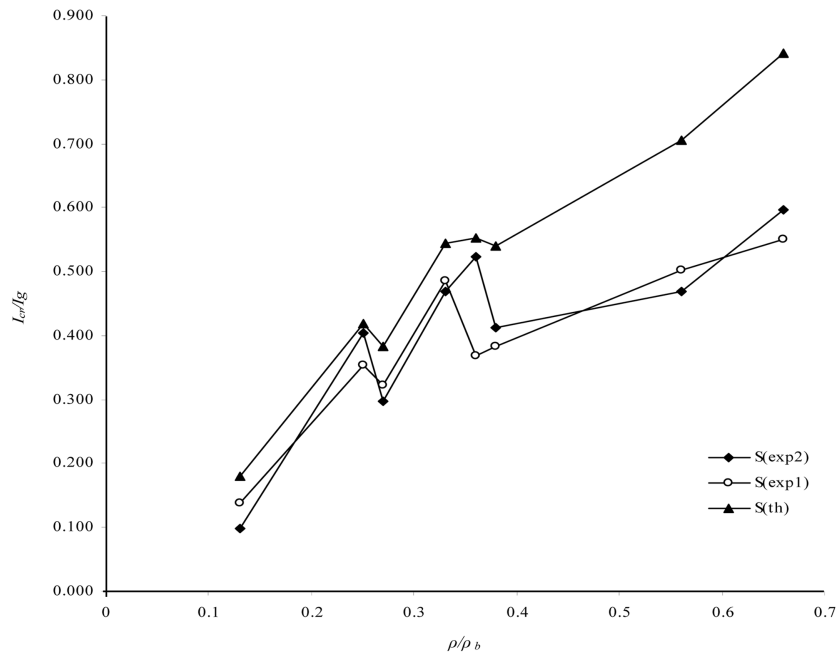
Fig. 10(a) Effect of $\rho$ on the $I_{cr}$ for tested members (S series)
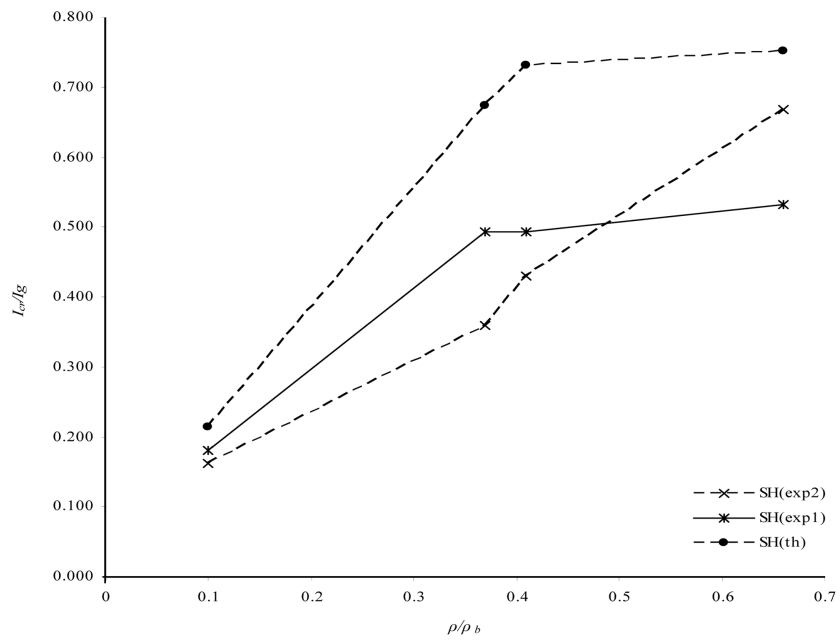


Fig. 10(b) Effect of $\rho$ on the $I_{cr}$ for tested members (HS series)

Table 9 The Experimental values of deflection, concrete compressive strain and crack width of tested members

| Member No. | $\Delta_{yi}$ (mm) | $\Delta_{yf}$ (mm) | $\varepsilon_{cyi}$ | $\varepsilon_{cyf}$ | $w_{cri}$ (mm) | $w_{cri}$ (mm) |
|---|---|---|---|---|---|---|
| S1 | 8.66 | 106.96 | 0.00084 | 0.01113 | 0.52 | 7.6 |
| S2 | 8.21 | 90.94 | 0.00099 | 0.01222 | 0.5 | 7.5 |
| S3 | 11.06 | 99.06 | 0.00101 | 0.01234 | 0.53 | 9.1 |
| S4 | 9.18 | 103.61 | 0.00182 | 0.01115 | 0.45 | 8.2 |
| S5 | 10.06 | 101.42 | 0.00291 | 0.01028 | 0.44 | 6.1 |
| S6 | 15.75 | 54.55 | 0.00341 | 0.00441 | 0.52 | 3.6 |
| S7 | 9.21 | 15.51 | 0.00125 | 0.00317 | 0.52 | 5.2 |
| S8 | 12.82 | 16.98 | 0.00163 | 0.00630 | 0.63 | 3.2 |
| SH1 | 5.52 | 33.63 | 0.00096 | 0.00437 | 0.64 | 2.5 |
| SH2 | 11.45 | 28.39 | 0.00451 | 0.00536 | 0.63 | 6.5 |
| SH3 | 14.01 | 15.14 | 0.00368 | 0.00911 | 0.58 | 4.2 |
| SH4 | 11.31 | 58.83 | 0.00536 | 0.01534 | 0.64 | 5.1 |

percentage of $\rho$, the value of $I_{cr}$ is increased. Also, (except for specimen S8$_{(th)}$), by comparing the results of the S$_{(exp)}$ with the S$_{(th)}$ it is obvious that, the values of $I_{cr}$ are higher than the obtained values of SH$_{(th)}$.

## 4. Beams behavior at initial and final horizontal plateau of yield stress

For the tested members the experimental values of deflection, concrete compressive strain and cracks width at initial ("*i*") and final ("*f*") yield plateau load are measured and shown in Table 9. At service conditions for NSC and HSC members, the allowable values of force in tensile bars, according to the Codes (ACI-318 2005, BS-8110 1985, CSA 1994), are lower than the yield values. To show the effect of high strength of concrete (in SCC) on deflection, compressive strain, and the width of crack of members, the rebar are tested in tension and the values at the beginning and final horizontal plateau of the steel stress-strain diagrams are determined and used here.

From the Table following important results can be drawn;

i) For all cases (except S6 and SH3), the deflection at initial yield plateau is less than 12 mm.

ii) Except for specimens S5 and S6, SH2-SH4, the values of $\varepsilon_{cyi}$ is approximately half the value of $\varepsilon_{cu} \approx 0.0035$ (suggested by CSA). As expected, the effect of $\rho'$ is to reduce the value of $\varepsilon_{cyi}$. Except for member S7, the values of $\varepsilon_{cyf}$ are higher than the values of 0.0035 and 0.003 recommended by CSA and ACI codes. In other words, the average value of $\varepsilon_{cyf}$ for tested members is 0.0088 which is 2.5 and 2.9 times the predicted codes values respectively, which is a good sign for ductility considerations in seismic regions.

## 5. Conclusions

Self-compacting concrete was developed and to be used mainly for highly congested reinforced concrete structures. The serviceability of reinforced concrete connections consisting of two types of

SCC were investigated, and the applicability for conventional vibrated concrete, as for ACI, BS and CSA code, was verified for SCCs members tested. The major conclusions derived from this experimental and theoretical study are given as follows:

1. Significant stages in load-deflection behavior of this type of concretes are their similarity in behavior with conventional concrete.

2. The applicability of crack width Equations for conventional normal strength concrete, as per ACI-318, BS-8110 and CSA code, was verified for SCCs members tested and it was found that; for a crack width 0.1 mm, the measured experimental crack width were very close to the predictions by British standard and ACI code respectively (except member, SH3). Considering crack width of 0.2 mm; comparison of the experimental results indicated that, the predictions of Eq. (3) were close to the values of $(\omega_{cr})_{exp}$ for connections (S4, S5, SH3), and for other 9 members the values of $(\omega_{cr})_{th}$ were smaller than $(\omega_{cr})_{exp}$. For Eq. (2) the calculated values of $(\omega_{cr})_{th}$ are smaller than the measured values of $(\omega_{cr})_{exp}$ (except SH3).

3. Assuming crack width 0.3 mm; again, the obtained theoretical values are smaller than experimental values as estimated after Eqs. (2) and (3), respectively.

4. In general, for almost all HSSCC members tested at the three levels of crack width (0.1, 0.2, 0.3 mm); the use of ACI Eq. (2) led to predict 33% of the results conservative (the ratio of $((\omega_{cr})_{th}/(\omega_{cr})_{exp})$ is greater than unity). However, considering Eq. (2) for the same levels of crack widths for NSSCC members, led to predict the unconservative results (the ratio of $((\omega_{cr})_{th}/(\omega_{cr})_{exp})$ is smaller than unity (except for S5 for crack width of 0.1 mm)).

5. The results of the BS Eq. (3) were noted to be conservative while compare to the ACI Eq. (2).

6. Considering CSA method; the quantity of "Z" for NSC members predicted for both interior and exterior exposure is applicable in SCCs members also. By use of a higher reinforcement ratio, the quantity of "Z" obtained is more conservative, and for the case of a lower reinforcement ratio, the obtained "Z" is closer to limiting values of CSA. The results are indicate that, although for interior exposure of S1 and SH3 members, the tensile steels reached the yield stress, but the crack widths were never increased more than limiting value of 0.4 mm even for the S1 specimen consisting of $\rho_{min}$ value.

7. For crack control, it is a usual practice to limit the value of tensile steel to $0.6f_y$. For this limiting value, the average crack width of tested members is 0.31mm which is lower than the suggested values for exterior and interior exposure of CSA method, for NSC members.

8. With SCCs, a very good bond is available between the bars and the surrounding concrete area of tested specimens.

9. A comparison between two Codes (ACI and CSA) for the theoretical values cracking moment is indicate that, irrespective of the concrete strength, for the specimens reported, the prediction values of two codes are almost equal.

In general, for all HSSCC members tested the use of two codes led to predict 50% of the results conservative (the ratio of (the ratio of $M_{cr})_{th}/(M_{cr})_{exp}$ is greater than unity), and for NSSCC, it led to predict unconservative results for 37.5% and 62.5% of the results (the ratio of $M_{cr})_{th}/(M_{cr})_{exp}$ is respectively greater and smaller than unity).

10. For all the cases, the values of $I_{cr(exp)}$ are lower than the values of $I_{cr(th)}$, and the values of $I_{cr(exp1)}$ are closer to the $I_{cr(th)}$ and higher than the values of $I_{cr(exp2)}$, except the specimens S4, S6, SH2. Also, a general conclusion is that, by increasing the percentage of $\rho$, the value of $I_{cr}$ is increased. Except for specimen $S8_{(th)}$, by comparing the results of the $S_{(exp)}$ with the $S_{(th)}$ it is obvious that, the values of $I_{cr}$ are higher than the obtained values of $SH_{(th)}$.

## References

ACI Committee 363 (1992), *Review of ACI Code for Possible Revisions for High-strength Concrete (ACI 362R-92)*, American Concrete Institute, Detroit.

Akbarzadeh Bengar, H. (2004), "Effect of tensile and compressive reinforcement ratio on ductility and behavior of high-strength concrete reinforced flexural members", M.Sc. Thesis, Department of Civil Engineering, University of Kerman, Iran.

American Concrete Institute (ACI) (2005), *Building Code Requirements for Structural Concrete and Commentary*, ACI 318-05 and ACI 318R-05.

Ashour, A.A. (2000), "Effect of compressive strength and tensile reinforcement ratio flexural behavior of high-strength concrete beams", *Eng. Struct.*, **22**(5), 413-423.

Bosco, C., Carpinteri, A. and Debernardi, P.G. (1990), "Minimum reinforcement in high-strength concrete", *J. Struct. Eng.-ASCE*, **116**, 427.

British Standard (1985), *Structural Use of Concrete*, BS8110, part2, London, UK.

Burns, N.H. and Siess, C.P. (1962), "Load-deformation characteristics of beam-column connections in reinforced concrete", *Civil Engineering Studies*, No.234.

Carrasquillo, R.L., Nilson, A.H. and Slate, F.O. (1981), "Properties of high strength concrete subject to short-term loads", *J. Am. Concrete Institute*, **3**, 171-178.

CSA 94 (1994), "CSA technical committee", *Design of Concrete Structure for Building*, CAN3-A23.3-M94, Canadian Standards Association, Rexdale, Ontario.

Ernst, G.C. (1957), "Plastic hinging at the intersection of beams and columns", *ACI J.*, **28**, 1119-1144.

Gatteh, H.F. (2006), "Experimental and theoretical investigation of reinforced self compacting concrete joints", M.Sc. Thesis, Department of Civil Engineering, University of Kerman, Kerman, Iran.

Ghali, A. (1993), "Deflection of reinforced concrete members, a critical review", *ACI Struct. J.*, **90**, 364-373.

Joint ACI-ASCE Committee 352 (2004), *Recommendations for Design of Slab-column Connections in Monolithic Reinforced Concrete Structures (ACI 35. IR-89)* (Reaproved 20004), American Conconcrete Institute, Farmington Hills, MI.

Khayat, K.H. (1999), "Workability, testing, and performance of self- consolidating concrete", *ACI Mater. J.*, **96**(3), 349-353.

Khayat, K.H., Paultre, P. and Tremblay, S. (2001), "Structural performance and in-place properties of self-consolidating concrete used for casting highly reinforced columns", *ACI Mater. J.*, **98**, 371-378.

Leslie, K.E., Rajagopalan, K.S. and Everard, N.J. (1976), "Flexural behavior of high-strength concrete beams", *ACI Struct. J.*, **73**, 517.

MacGregor, J.G. and Wight, J.K. (2005), *Reinforced Concrete Mechanics and Design*, 4th Edition, Pearson Prentice Hall, Upper Saddle River, New Jersey.

Maghsoudi, A.A. and Akbarzadeh Bengar, H. (2005), "Effect of $\rho'$ on ductility of HSC members under bending", *Proceedings of the 7th International Symposium on Utilization of High-Strength/High Performance Concrete*, Washington, D.C., USA.

Mansur, M.A., Wee, T.H. and Chin, M.S. (1994), "Some engineering properties of locally produced high-strength concrete", *Proceedings of the 19th Conference on Our World in Concrete and Structures*, CI-Premier Pte. Ltd., Singapore.

Mohamadi, Y.M. (2007), "Behavior of high strength self compacting concrete joints under load", M.Sc. Thesis, Department of Civil Engineering, University of Kerman, Kerman, Iran.

Mohammad, L., Khadaker, M., Hossain, K.M. and Vasilios, B.L. (2006), "Axial load behavior of self-consolidating concrete-filed steel tube columns in construction and service stages", *ACI Struct. J.*, **2**, 57-65.

Nilson, A.H. (1987), "Design implication of current research on high strength concrete", High-Strength Concrete, ACI SP-87, American Concrete Institute, Detroit.

Okamura, H. (1997), "Self-compacting high-performance concrete", *Concrete Int.*, **19**(7), 50-54.

Pateli, R., Hossain, K.M., Shehata, M., Bouzabaa, N. and Lachemi, M. (2004), "Development of statistical models for mixture design of high-volume fly ash self-compacting concrete", *ACI Mater. J.*, **101**, 294-302.

Rashid, M.A., Mansur, M.A. and Paramasivam, P. (2002), "Correlations between mechanical properties of high-strength concrete", *J. Mater. Civil Eng.*, **3**, 230-238.

Robertson, I.N., Kawai, T., Lee, J. and Enomoto, B. (2002), "Cyclic testing of slab-column connections with shear reinforcement", *ACI Struct. J.*, **99**(5), 605-613.

Saria, M., Prat, E. and Labastire, J.F. (1998), "High-strength self-cmpacting concrete, original solutions associating organic and inorganic admixtures", *Proceedings of the International Symposium on High-Performance and Reactive Powder Concretes*, University of Sherbooke.

Skarendahl, A. and Petersson, Ö. (2001), "State-of-the-art report of RILEM technical committee 174-SCC", Self-Compacting Concrete, Report No.23, 141.

Sonebi, M. and Bortos, P.J.M. (2001), "Performance of reinforced columns with self-compacting concrete", *Proceedings of the 5th CANMET/ACI International Conference*, American Concrete Institute, Farmington Hills.

Swamy, R.N. (1987), "High strength concrete-material properties and structural behavior", High-Strength Concrete, ACI SP-87, American Concrete Institute, Detroit.

Yurugi, M. (1998), "Application of self-compacting concrete in japan", *Proceedings of the 23rd OWICS Conference*, Singapore.

## Notations

$a$     : shear span
$a'$    : distance from extreme concrete compressive fiber to point that calculate crack width
$A_s$   : area of logitudinal tension reinfocement
$A_s'$  : area of logitudinal compresion reinfocement
$b$     : width of beam
$c$     : concrete cover
$C$    : experimental constant
$d$     : effective depth
$d_c$   : distance from extreme tensile concrete fiber to the center of the nearest tension bars
$h$     : height of beam
$E_c$   : modulus of elasticity of concrete
$E_s$   : modulus of elasticity of steel reinforcement
$f_c$    : concrete compressive stress
$f_c'$   : concrete compressive strength
$f_r$    : modulus of rupture for concrete
$f_y$    : steel yielding stress
$h_1$   : distance from neutral axis to area center of tension reinforcement
$h_2$   : distance from neutral axis to extreme concrete tensile fiber
$I_{cr}$   : moment of inertia of cracked transformed section
$I_e$    : effective moment of inertia
$\varepsilon_{cy}$   : the measured compression strain in the concrete at yielding of steel reinforcement.
$\varepsilon_{sy}$   : the measured tensile strain in steel reinforcement at yielding stage
$x$     : neutral axis depth
$P_y$   : the load that causes yielding in the steel reinforcement
$l$     : the clear span of the member
$i_{cr}$    : can also be defined as the slope of the line connecting the origin and point of initial yielding of tensile reinforcement in moment curvature curve
$y_t$    : the neutral axis depth measured from bottom side of the member
$f_s$    : tensile reinforced stress under service load
$M_a$   : maximum moment in the beam at a stage at which deflection is computed
$M_{cr}$  : cracking moment of beam